Low cost time division multiplexing of identical optical fibre ring intensity sensors

R. Fernández de Caleya, M. López-Amo and J. A. Martín-Pereda

A time division multiplexing (TDM) array for passive multiplexing of identical fibre optic intensity sensors has been demonstrated. Microbending loss sensors are introduced in fibre optic rings and pressure information is directly detected, demultiplexed and demodulated from the relative amplitude of the first two pulses produced on each ring. Several dynamic ranges from 6 dB to 14 dB are shown. A comparison between both fibre optic ring and Mach–Zehnder structure impulse responses is carried out and the consequences derived from second- and higher-order recirculating ring pulses are also evaluated. This technique can be applied to those TDM intensity sensing schemes which require low cost, high number of identical sensors, and suffer high element loss and undesirable intensity fluctuations at low frequencies.

1. Introduction

In some applications, physical parameters can be directly registered in the optical intensity of the light along an optical fibre. Intensity sensors offer enough dynamic range to detect and measure sensing information. They can be implemented with both single-mode or multimode optical fibres. Light emitting diodes (LEDs) or laser diodes (LDs) are suitable as optical sources. Intensity sensors represent a lower cost solution when compared to optical interferometric sensors. However, intensity fluctuations due to optical sources or produced in the transmitting optical fibres, and the difficulties in multiplexing them on an array, have contributed to reducing their practical applicability. In fact, information registered in the amplitude of a single pulse is exposed to undesirable light perturbations. If these intensity sensors are included in time delay structures, such as recirculating ring or non-recirculating Mach–Zehnder configurations it is possible then to integrate several intensity sensors on a single array and recover the sensing information without any undesirable low frequency amplitude fluctuation.

In this work, a novel time division multiplexing method for integrating a high number of intensity based sensors is presented. Several topologies are also discussed. Pulsed light is used and microbending loss sensors are applied along the length of optical fibre rings. In this way, pressure information is dirctly registered as external loss in the amplitude of the first and the successive recirculating pulses generated from each of the rings. If an adequate ring coupling constant is chosen, this sensing information can be detected and measured from the relative amplitude of the reference and the first recirculating pulses, which provides an improved dynamic range. The optimum coupling constant value depends on the coupler excess loss and the recirculating length loss of the fibre. We demonstrate that sensing dynamic range is inversely proportional to this value and the intrinsic excess loss of the rings. Minimum threshold detection level of the photodetector is also taken into account in this analysis. Mach–Zehnder and ring structures are compared and evaluated in a ladder array. Experimental results are shown in this work to verify the behaviour of the theoretical analysis.

Received 2 June 1993; revision received 15 November 1993.

Authors' address: Departamento de Tecnología Fotónica, E.T.S.I. Telecomunicación, Universidad Politécnica de Madrid, Ciudad Universitaria s/n, 28040-Madrid, Spain.

2. Impulse response of optical fibre intensity sensing structures

The intensity sensing structure considered initially is an optical fibre crosscoupled ring (CCR) where a microbending loss sensor is applied in the recirculating loop, as shown in figure 1(*a*). Other intensity sensors [1, 2] could be also applied in that structure, but we will limit

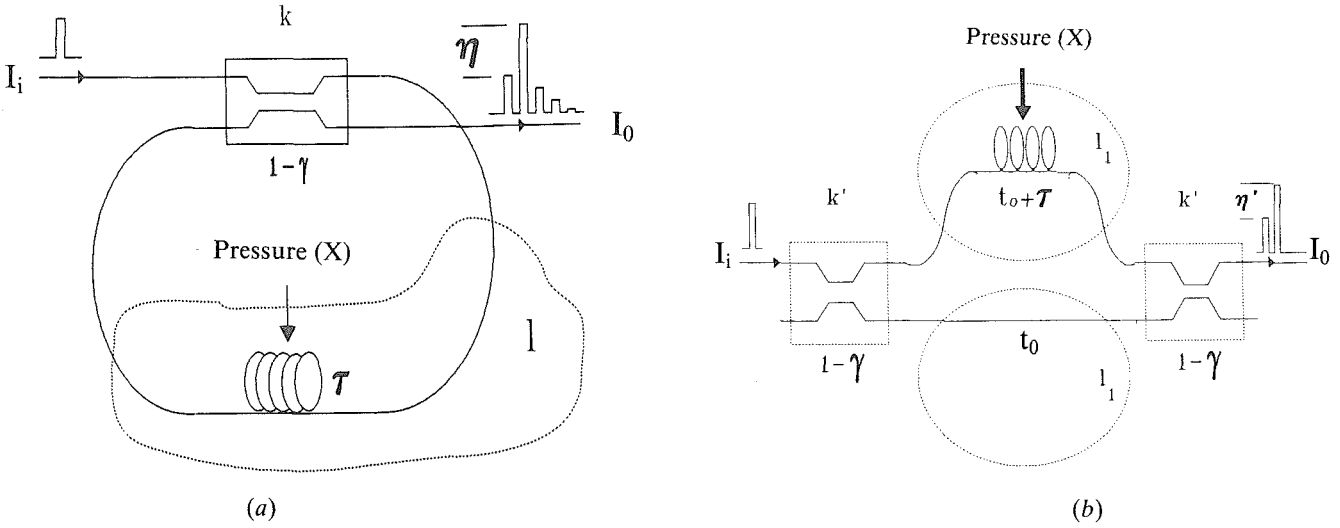

Figure 1. Optical fibre intensity sensor structures: (*a*) ring structure; and (*b*) Mach–Zehnder structure.

our analysis to those sensors that detect external loss measurements directly proportional to the applied external pressure. In such structures, β is the intrinsic excess loss per complete recirculation of the ring. This parameter assembles the coupler insertion loss (γ) and the intrinsic loop loss due to connectors, splices and propagation in the fibre (l). The variable external microbending loss applied to the loop, which is the physical parameter to be measured, will be called X. If k is the power coupling constant of the directional coupler, and τ is the time delay per recirculation in the ring, the time domain intensity response can be expressed as follows:

$$h_{CCR}(t)=(1-\gamma)k \times\left\{\delta(t)+\eta\sum_{i=0}^{\infty}\left[\eta\left(\frac{k}{1-k}\right)^2\right]^i\delta(t-(1+i)\tau)\right\}, \tag{1}$$

where η is the ratio between the first recirculating pulse amplitude and the non-recirculating pulse amplitude, being defined by

$$\eta=\eta_0 X=(1-\gamma)l\frac{(1-k)^2}{k}X=\beta\frac{(1-k)^2}{k}X. \tag{2}$$

As external losses are lower or equal to unity ($X\leqslant 1$) when the value of the coupling constant is much smaller than unity ($k\ll 1$), and no gain is applied to the fibre loop, then the coefficients in the summation in (1) are also much smaller than unity due to

$$\eta\left(\frac{k}{1-k}\right)^2=\beta k X\ll 1. \tag{3}$$

Consequently, since these coefficients are raised to the power of i, all terms of the summation tend exponentially to zero except for $i=0$. On the other hand, the coefficient of the second term, for $i=0$, increases drastically as k approaches zero, assuming no external losses are applied ($X=1$). This is equivalent to saying that when the coupling constant value tends to zero, the optical power of the first recirculating pulse normalized to that of the non-recirculating pulse (also called the reference pulse) increases exponentially. Therefore, we can compare the optical powers of the reference and the first recirculating pulses to those from the rest of the recirculating pulses produced in the ring. Using the coefficients of (1) and supposing that $X=1$, this magnitude can be represented as a power ratio (PR) given by

$$\mathrm{PR}=\frac{1+\eta_0}{\eta_0\sum_{i=1}^{\infty}\left[\eta_0\left(\frac{k}{1-k}\right)^2\right]^i}. \tag{4}$$

This ratio gives the relative power in the reference and the first reciruclating pulse compared to the total optical power from the remaining pulses. In figure 2(*a*), the parameter PR is plotted for small values of k considering various values of β and assuming that $X=1$. It is shown for $\beta=0$(–), -1(––), -3(–·) and -6(···) dB that intrinsic losses enlarge the relative energy of two such first pulses compared to the rest. This effect is much more evident when the coupling constant approaches zero.

From the previous results it is observed that, in a CCR structure, if the coupling constant value, k is much lower than 1 ($k\ll 1$), most of the transmitted power is concentrated in the first recirculating pulse, being negligible in the second and successive recirculating pulses. When k approaches zero, the value of the

parameter η_0 can be much larger than unity, even if internal loss, β, has practical values. As can be deduced from (2), the relative difference between the first two pulses generated in the ring increases.

Since intensity fluctuations produced out of the ring affect of all these pulses in the same proportion the ratio between the first recirculating pulse and the reference pulse (which can be considered to be the demodulated signal value of η) will be free of such perturbations, being only dependent on the external losses applied on the ring. This means that X would be the exact magnitude being detected when external pressure is applied to the loop. The dynamic range of the detected signal could be defined as the maximum excursion of the normalized signal, η. It is reasonable to take as the amplitude of the reference pulse A_1 the minimum amplitude detectable from the photodetector, this value is discussed below. Thus, if the value of X is equal to $1/\eta_0$, the amplitude of the first recirculating pulse A_2 becomes identical with A_1. In that case, it is defined as the minimum detectable value. On the contrary, when no pressure is applied, no external loss is detected and, therefore, X is equal to unity. Once both limits have been defined, the dynamic range DR of the normalized amplitude A_2/A_1 can be written as

$$\mathrm{DR}=\left|\frac{A_2}{A_1}(X=1)-\frac{A_2}{A_1}\left(X=\frac{1}{\eta_0}\right)\right|=\eta_0-1. \quad (5)$$

In figure 2(b), the normalized parameter $\eta=A_2/A_1$ is plotted versus X. The corresponding values of DR for several values of β are also shown. From these curves, it is easy to check that the dynamic range is a linear function of the external applied loss X with a slope equal to η_0. Therefore, the maximum value of DR is achieved for a maximum value of η_0.

Ideally, η_0 could converge to infinity, but, in a real system, the value of the reference pulse should be adjusted to the minimum detectable amplitude of the detector plus a saving margin determined by the maximum absolute fluctuations allowed in the system. We can normalize these intensities to the input pulse amplitude I_i and call them U and M, respectively. Hence, the lower bound of k, $k_{\min}$, is given by

$$k_{\min}=\frac{U+M}{(1-\gamma)}. \quad (6)$$

From this result, the value of η_0, particularized to $k_{\min}$ is the maximum value obtainable. The value of the detected X is bounded between

$$\text{max. external loss detectable:}\frac{U+M}{(1-\gamma)^2 l\left(1-\dfrac{U+M}{1-\gamma}\right)^2}\leqslant X\leqslant 1\text{: no external loss applied,} \quad (7)$$

where the lower bound relates to the maximum detectable external loss and the upper bound to no applied external loss.

The intensity sensor can also be introduced into one of the two branches of an optical fibre Mach–Zehnder

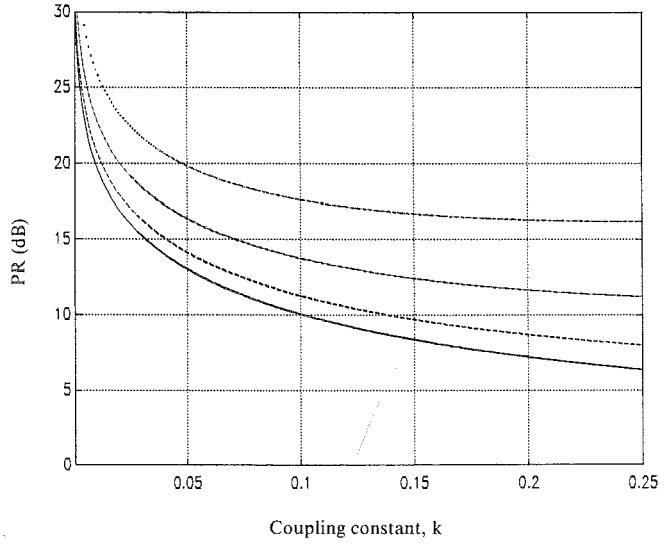

(a)

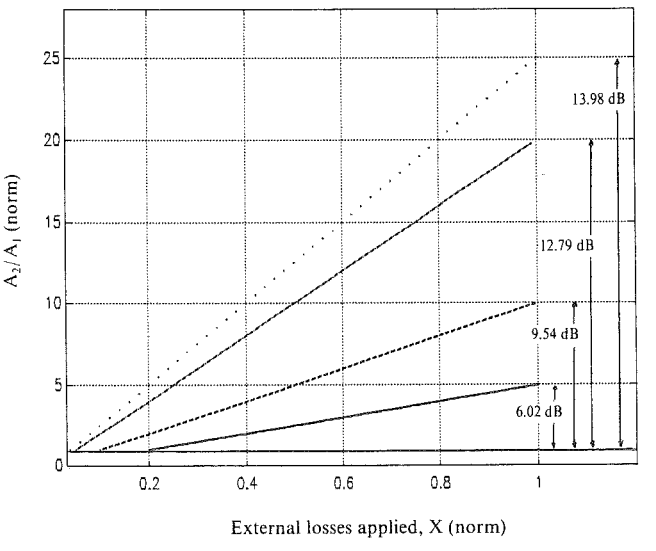

(b)

Figure 2. **(a) Optical power ratio between the reference plus the first recirculating pulse, and the second and higher order pulses, PR, versus the coupling constant of the ring, k. Curves correspond to the values of $\beta=0$ [–], -1 [– –], -3 [– ·] and -6 [· · ·] dB; (b) the normalized parameter η versus the external loss applied (X). The dynamic range, DR, of this sensor structure is also shown for the following values of $\eta_0=5$ [–], 10 [– –], 20 [– ·] and 25 [· · ·].**

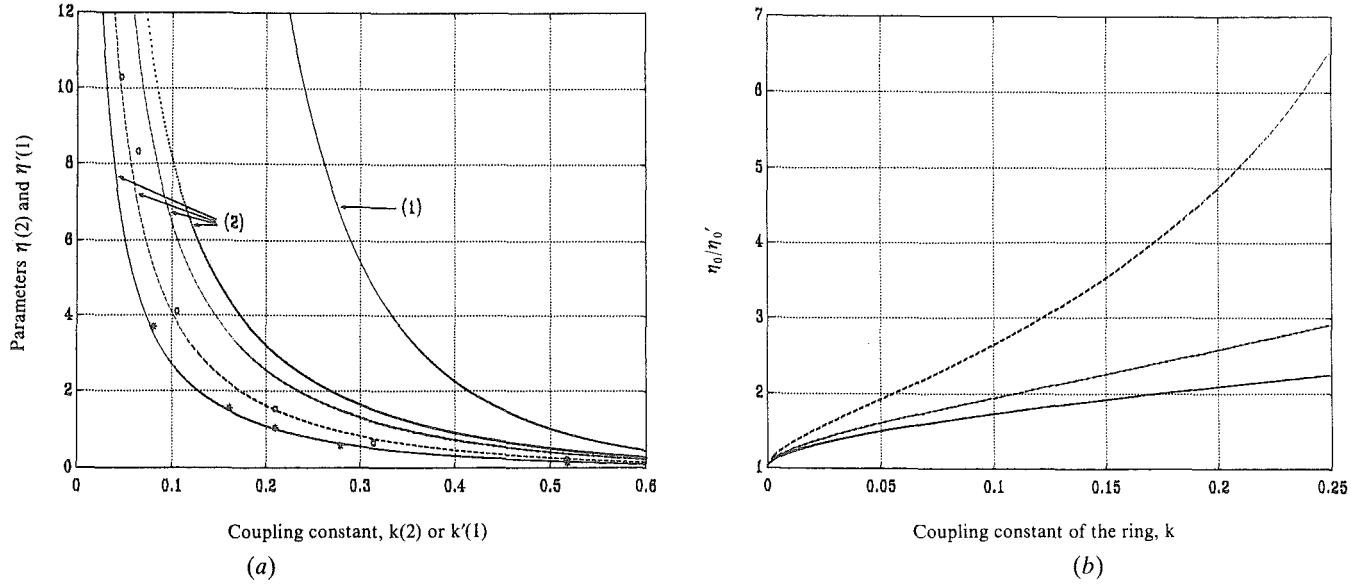

Figure 3. (*a*) **Parameter η' versus k' for a Mach–Zehnder structure (curve called 1), and parameter η versus k for a ring structure (curves called 2) with several total recirculating losses ($\beta=0$ [···], -1 [–·], -3 [– –] and $-4{\cdot}77$ [–] dB). Plotted points [○] and [*] are experimental results when $\beta=-3$ and $-4{\cdot}77$ dB, respectively; (*b*) η_0/η_0' versus the coupling constant of the ring (k), when the reference pulses of the ring and the Mach–Zehnder structure are identical. Values of β considered are 0 [–], -1 [–·] and -3 [– –] dB.**

(MZI) structure, using the other one as a reference. In this configuration, two coupliers are required instead of the single coupler needed in a ring structure. As was shown above, if the coupling constant of the ring is close to zero, sensing information can be extracted from the first two pulses. In that case, both structures can be compared [3]. In order to accomplish this fact, both directional couplers have been considered with identical coupling constant k', having an excess loss value of γ. The differential time delay between the two branches is τ. The intrinsic loss per branch is considered identical and equal to l_1 when the propagation fibre loss along τ is neglected. In that case, for the scheme shown in figure 1(*b*), the intensity impulse response for the Mach–Zehnder structure is given by

$$h_{\mathrm{MZI}}(t)=(1-\gamma)^2(k')^2 l_1\{\delta(t)+\eta'\delta(t-\tau)\}. \qquad (8)$$

Now, the new parameter η' is the ratio between the amplitudes of the second and the first pulses. This corresponds to the demodulated signal and is expressed as

$$\eta'=\eta_0' X=\left(\frac{1-k'}{k'}\right)^2 X. \qquad (9)$$

The values of η_0 and η_0', depending on k and k', respectively, have been plotted in figure 3(*a*) for different values of $(1-\gamma)$ and l. For the curves in which total intrinsic excess loss is -3 dB (○) and $-4{\cdot}77$ dB (*), plotted points, (○) and (*), correspond to experimental measurements on the ring configuration. It is shown that the same value for parameters η_0 and η_0' can be obtained for different values of the corresponding coupling constants, and always when $k<k'$. As assumed above, since the loss produced by intrinsic propagation in the fibre differential length (with delay τ) has been neglected, η_0' depends exclusively on k'. Being now the dynamic range equal to $\eta_0'-1$, this value is maximized when η_0' increases. In order to compare such structures, both Mach–Zehnder and ring reference pulse amplitudes can now be designed to be identical. This occurs when k and k' are related by

$$k=(1-\gamma)l_1(k')^2. \qquad (10)$$

In this case, the efficiency of both structures is easily determined by calculating the ratio η_0/η_0'. Taking (10) into account, this ratio has been plotted in figure 3(*b*) versus the coupling constant of the ring for several values of β. As shown, the DR of the ring is always greater than the DR of the Mach–Zehnder structure. It is also observed that η_0 is larger than η_0', the difference being more accentuated when both loop loss and k increase.

Therefore, when an intensity sensor is introduced in a multibranch fibre structure, information can be registered as an external loss and detected without undesirable amplitude fluctuations due to optical power fluctuations in the system. For a given intrinsic loss in the

structures considered, the dynamic range is dependent upon their coupling constants. The first two transmitted pulses of the ring stucture have been compared with those produced in the Mach–Zehnder structure, when values of k are close to zero. For these values, the largest part of the power is concentrated in the first two pulses, and a larger dynamic range is achieved with the ring configuration. Furthermore, a real limitation of the minimum threshold detection level of the photodetector is also considered in the evaluation of the minimum coupling constant of the ring.

3. Time division multiplexed sensing array

Time division multiplexing of the sensing structures, which has been characterized in the previous section, is achieved by using a pulsed LED or LD source. Since transmitting structures are chosen, periodic pulses emitted from the source are launched to and derived from the sensing array by input and output buses, respectively. The topology analysed is a transmitting ladder array in whch N sensing rings are located on the ladder steps along the two buses. Directional couplers used to link the same step between buses are identical and their coupling constants are tailored along the steps of the buses to ensure equal optical power returning from each sensor at the output bus.

As shown in figure 4, $S_1, S_2, \ldots, S_N$ are the microbending intensity based sensors, $k_1, k_2, \ldots, k_N$ are the tailored coupling constants of the array, γ is the excess loss per coupler, and $T_1 = T_2 = \cdots = T_N = T$ are the fixed identical delays between sensing steps. This value is an integer number of τ, and is crucial for determining the crosstalk of the array. Propagation losses along the fibre are neglected in the following analysis. Coupling constants of the bus couplers are tailored to achieve

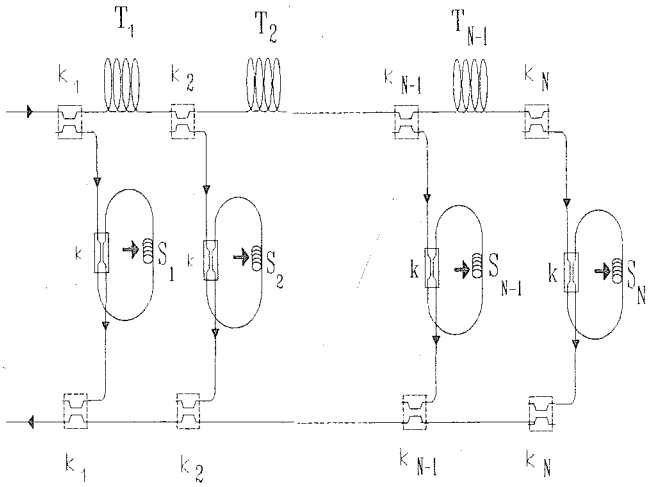

Figure 4. Intensity sensor ladder array formed from optical fibre ring structures.

identical optical power from each sensor at the output bus head. The coupling constants of adjacent couplers are then related by

$$k_{j+1} = \frac{1}{(1-\gamma)} \frac{k_j}{1-k_j}. \tag{11}$$

Considering $k_N = 1$ and after some algebra as in references 4 and 5, the optimum coupling value of the jth-coupler, when coupler losses ($\gamma \neq 0$) and N sensors are considered, is

$$k_j = \gamma \frac{(1-\gamma)^{N-j}}{1-(1-\gamma)^{N-j+1}} \quad \forall j \tag{12}$$

and, for the lossless case ($\gamma = 0$),

$$k_j = \frac{1}{N-j+1} \quad \forall j. \tag{13}$$

From these values, the optical power at the output bus due to the first recirculation of each ring, normalized to the input pulse I_i, can be found to be

loss case:

$$I_s^1 = (1-\gamma)^4 \left(\frac{\gamma(1-\gamma)^{N-1}}{1-(1-\gamma)^N} \right)^2 l(1-k)^2 X, \tag{14a}$$

lossless case:

$$(l=1, \gamma=0): \quad I_s^1 = \frac{(1-k)^2}{N^2} X. \tag{14b}$$

These expressions are calculated considering the first sensor. However, because of the tailoring given by (12) and (13), the optical power of each pulse at the output bus is identical for any of the sensors in the network. The returned optical power normalized to I_i for the reference pulse is calculated in the same way, being now

loss case:

$$I_s^r = (1-\gamma)^3 \left(\frac{\gamma(1-\gamma)^{N-1}}{1-(1-\gamma)^N} \right)^2 k = \xi k, \tag{15a}$$

lossless case:

$$I_s^r = \frac{k}{N^2}. \tag{15b}$$

Maintaining the same ladder network, identical values for $k_1, k_2, \ldots$ and k_{N-1} could be obtained by changing the ring structures to Mach–Zehnder structures. Therefore, when these structures are inserted in the array, the relation for the second transmitted optical pulse of the structures at the output bus are the same as for the ring structures ((14 a) and (14 b)), but now with k' and l_1 replaced by k and l, respectively. In the same way, the returned optical power from the reference pulse is given by (15 a) and (15 b), with k

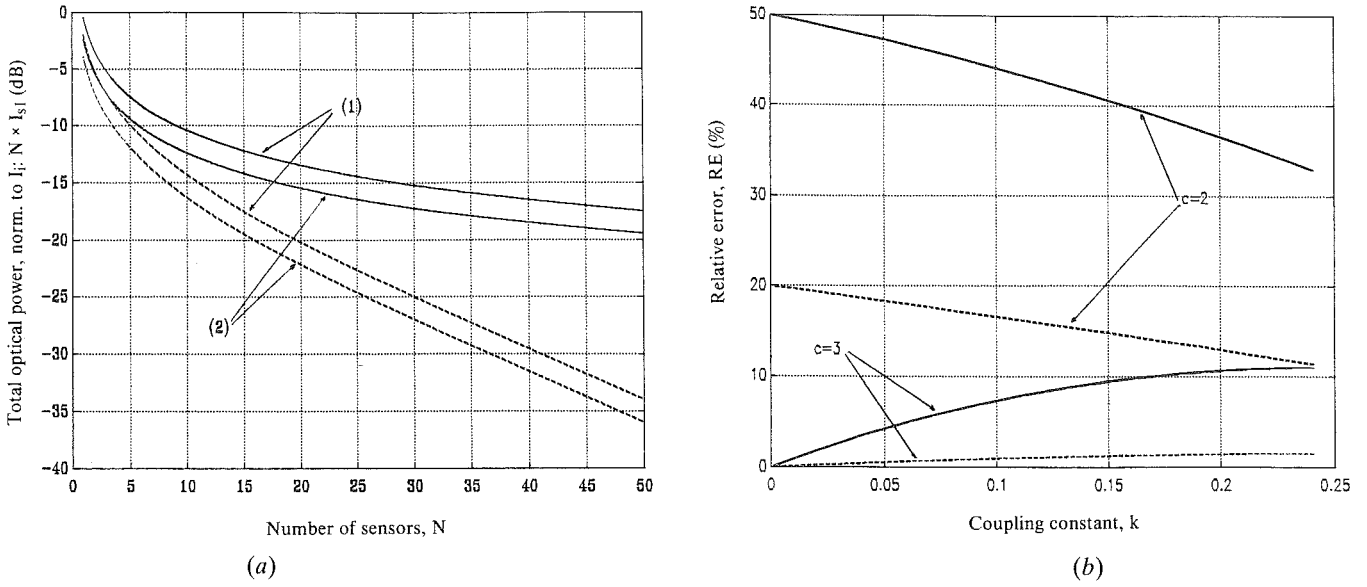

Figure 5. **(*a*) Total optical power returned at the output bus due to the second pulse produced in the structures and normalized to the input optical power (NI_s^1) versus number of sensors (N). Loss case [––] corresponds to values of $(1-\gamma)$ equal to $-0{\cdot}25$ dB and 1 equal to $-0{\cdot}5$ dB, and lossless case is plotted as continuous line [–]. Structures considered on the array are rings (1) and Mach–Zehnders (2); (*b*) relative error, $RE(\%)$, versus the coupling constant of the rings, k, for $c=2$ and 3, and for $\beta=0$ [–] and -3 [––] dB. The fixed time delay between sensors is $T=c\tau$.**

replaced by k' and multiplying the loss case equation by $(1-\gamma)l_1$. In the following analysis, all losses per branch, l and l_1, will be considered identical.

The total returned optical powers corresponding to the first recirculating pulse in the ring and the informatin pulse in the Mach–Zehnder structure are expressed as functions of the number of sensors N multiplied by the power returned from the information pulse produced in each sensor $N\times I_s^1$. In figure 5(*a*) these functions are represented versus the number of sensors, for both the lossless case (ideal case) and loss case (non-ideal case). Curves obtained in this last case have been calculated for $(1-\gamma)=-0{\cdot}25$ dB and $l=-0{\cdot}5$ dB. Coupling constant of the couplers are considered to be $k=0{\cdot}05$ and, from (10), Mach–Zehnders coupling constants are $k'=0{\cdot}2429$. In that way, the dynamic range for both ring and Mach-Zehnder structures can be compared and their values are 11·52 and 9·40 dB, respectively, its being observed that $DR_{CCR}>DR_{MZI}$, as discussed above. It is inferred from these curves that ring ladder arrays are able to integrate a larger number of sensors when compared with Mach–Zehnder ladder arrays, when identical total returned optical power is assumed. Now, the value of k_{min}, calculated in (6), has to be modified to $k_{min}=(U+M)/\xi$, where ξ has been defined in (15 *a*) for the loss case, and $k_{min}=(U+M)N^2$ for the lossless case. Consequently, the value of the maximum external loss detectable is also decreased in the same proportion.

Once the values of the coupling constants are fixed, time delay T is determined by ensuring a low crosstalk between pulses and, simultaneously, by maintaining a not-too-high repetition input pulse period. Taking this fact into account, the total delay produced on the array for the jth-sensor is equal to $(j-1)c\tau$, where τ is the delay of the ring and c is an integer number greater than or equal to 2. For an N sensor array, like the one shown in figure 4, the repetition pulse rate of the source is $1/cN\tau$. Hence, the duty cycle is $1/c$, assuming that the first recirculating pulse is the only carrier of the sensor information. From this value for T, the information pulse of the jth-sensor only interferes significantly with the $(c+2)$th-pulse of the $(j-1)$th-sensor. As a matter of fact, those pulses might also interfere with the $(c+2m)$th-pulses of the $(j-m)$th-sensor, for an integer number of $m\geq 2$. But values of η_0 considered here are much larger than unity and, hence, the contribution of the interference pulses coming from non-adjacent sensors can be neglected. This means that interference pulses generated from the array associated with the information and reference pulses can be determined from the adjacent sensor. However, a possible problem emerges when the crosstalk function has to be defined from two different pulses. Since information and reference pulses represent the final normalized information amplitude and both pulses are associated with interference pulses at the output bus, η is redefined as a function of A_2 plus the interference produced by the

$(c+2)$th-pulse amplitude (A_{c+2}) divided by A_1 plus the interference produced by the $(c+1)$th-pulse amplitude (A_{c+1}). In this case, we have considered that the most important information about the effect of such interference (or crosstalk) has to be obtained from the normalized signal, measured at the output of the division circuit. Thus, the relative shift generated when interference pulses are considered associated with both such information and reference pulses can be calculated from the ideal case. The relative error RE produced from these added interference pulses associated with the respective amplitudes A_1 and A_2 to the ideal parameter A_2/A_1, is given by

$$\mathrm{RE}(\%) = \left| \frac{\dfrac{A_2 + A_{c+2}}{A_1 + A_{c+1}} - \dfrac{A_2}{A_1}}{\dfrac{A_2}{A_1}} \right| \times 100$$

$$= \left| \frac{1}{X_j} \left[\frac{X_j + X_{j-1}\left[\eta_0 X_{j-1}\left(\dfrac{k}{1-k}\right)^2\right]^c}{1 + \eta_0 X_{j-1}\left[\eta_0 X_{j-1}\left(\dfrac{k}{1-k}\right)^2\right]^{c-1}} \right] - 1 \right| \times 100, \quad (16)$$

where X_j and X_{j-1} are the external losses applied to the jth-sensor and the $(j-1)$th-sensor, respectively. In order to simplify the analysis of the relative error, we have considered that no external losses are applied and, hence $X_j = X_{j-1} = 1$. In figure 5(b), the relative error versus the coupling constant of the rings is shown for $c=2$ and 3 and for $\beta = 0$(–) and -3(– –) dB. When $c=2$ and no intrinsic losses are assumed, the reference pulse and the second recirculating pulse amplitudes for a value of k approaching zero are very close and, consequently, the error function obtained is unacceptably high. However, the amplitudes of the reference pulse and the third and successive recirculating pulses (for $c \geq 3$) diverge when k approaches zero. Hence, the error also approaches zero. As can also be obtained from the graph in figure 5(b), the intrinsic loss reduces substantially the relative error produced.

As an alternative to the ladder topology studied, intensity sensors could be integrated in a recursive lattice array or directly in the steps of the same non-recursive ladder array. Both arrays have been analysed in references 4 and 5, and it is shown that there is only one reference pulse per input optical pulse, resulting in the fact that if any loss is produced in the array, not all sensing information is correctly demodulated. Furthermore, loss in the buses or in the recursive lattice topologies increases drastically the network crosstalk. Hence, the number of sensors that can be deployed in these arrays is fairly limited.

4. Verification of the time domain behaviour

In order to check the feasibility of the calculations, we have implemented a non-recursive ladder array of two intensity ring sensors ($N=2$). The intensity time domain responses have been visualized on a digital oscilloscope via an optoelectronic converter with a sensitivity of $1\,\mathrm{V\,mW^{-1}}$. In this experiment, we have employed singlemode optical fibre, tunable directional couplers and a pulsed optical LD optical source stabilized at 1300 nm. The signals at the output of each ring are shown in figures 6(a) and 6(b), and the total detected signal is shown in figure 6(c). We have employed ring lengths of 8 m, being the ring coupling constants 0·061 and 0·062 for the first and the second ring, respectively, and $\beta\,(X=1) = -4{\cdot}77$ dB. The fixed time delay between sensors was 16 m ($c=2$). The coupling constants of the bus couplers were nominally 0·5. The minimum effect of the second recirculating pulse amplitude is observed for the values of the coupling constants given above, and for the large intrinsic excess loss admitted (-4.77 dB). As can be seen, the value of the dynamic range was not maximized for the optimum value of k. However, an almost inappreciable error function was obtained even for that value of k. This optimum value has to be higher when compared with the case of a single ring in the array. Therefore, the value of the measured dynamic range of the first ring at the output of the bus head (3·95 dB) is lower than that measured at the output of the ring (5·65 dB). This means that the optimum coupling constants of the rings are dependent on the array arrangement, as well as on the minimum threshold detection level of the photodetector. In that way, the dynamic range suitable for each sensor ring is achieved.

5. Conclusion

A time division multiplexing array of identical intensity sensing structures has been reported and analysed. Concerning the above mentioned system, two new improvements can be obtained from the information pulse amplitude, A_2, normalized to the reference pulse amplitude, A_1. First, any fluctuations in the optical power injected into the ring are cancelled from the information signal after such normalization. Secondly, the dynamic range is substantially increased. This is is an important advantage if a large number of sensors is to be deployed in the array.

The number of sensors does not essentially affect the crosstalk level. A relatively large dynamic range is easily obtained when physical parameters are directly proportional to the external losses applied to the loops.

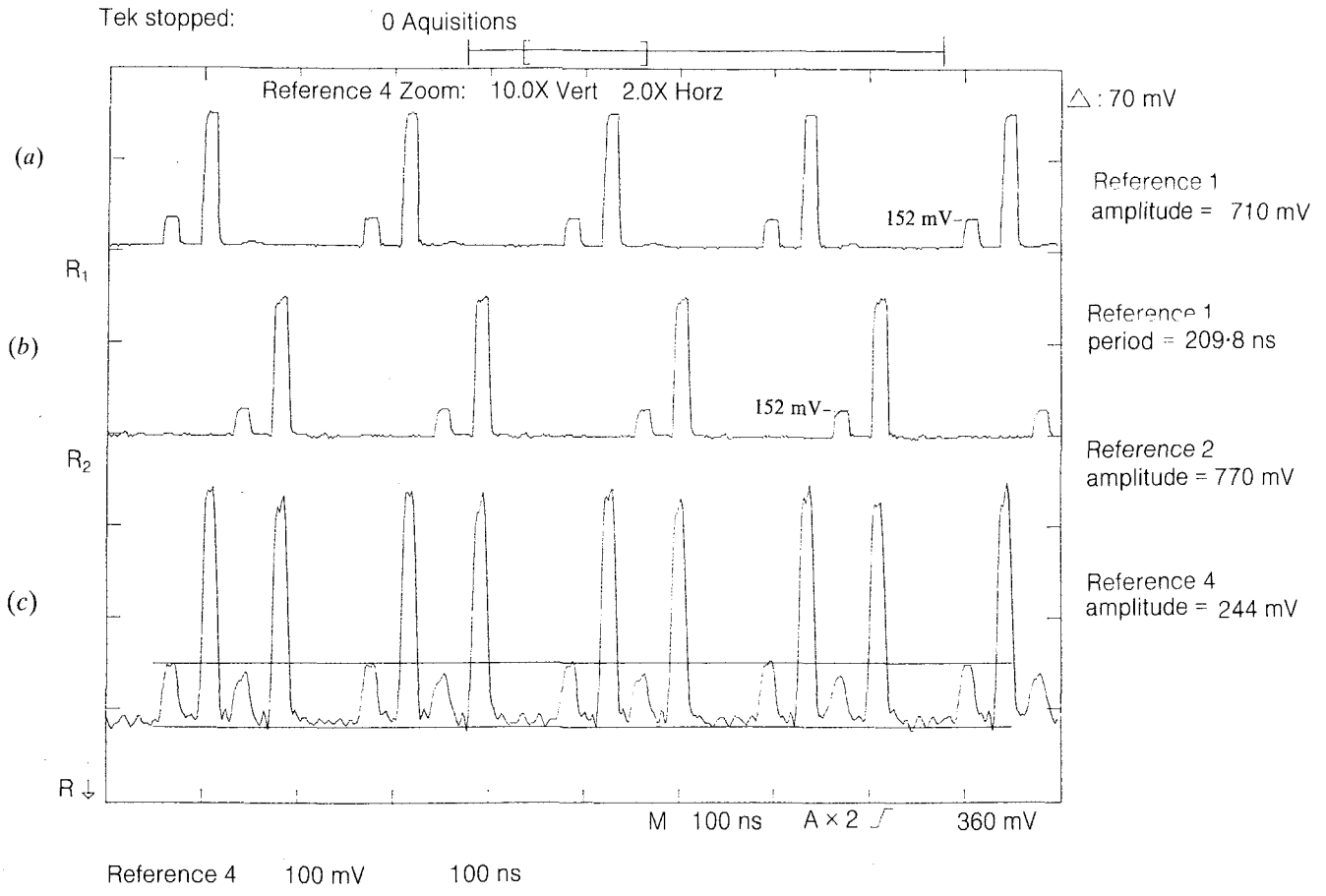

Figure 6. Time domain intensity responses of a two-sensors ladder array for $T=2\tau$, detected: (*a*) at the first sensor output; (*b*) at the second sensor output; (*c*) at the output bus head.

A large number of sensors can be integrated for a low detection threshold of the photodetector and an acceptable crosstalk level is achieved for a value of c larger or equal to three, independently of both the couplers and fibre losses of the buses. The intrinsic excess loss of the rings reduces drastically the error function of the normalized signal. No crosstalk is present when Mach–Zehnder structures are integrated in the array. This fact is due to their non-reeursive nature. However, the price to pay is a lower dynamic range and a lower level of total optical power. This means that, for the same power levels, the number of sensors is decreased. Furthermore, ring structures are easier to implement and they only require one coupler per structure. Experimental results confirm the feasibility of the reported sensing network.

Acknowledgments

The authors wish to thank to J. L. Santos from INESC (Porto, Portugal) for his helpful discussions and commentaries. This work has been supported by Spanish CICYT (TIC-211/89, TIC.92-0052-C02 and TIC-1232/93-E).

References

[1] Jackson, D. A., and Jones, J. D. C., 1986, *Optica Acta*, **33**, 1469.

[2] Culshaw, B., and Dakin, J., (editors), 1989, *Optical Fibre Sensors*, Vols 1 and 2 (Norwood, Mass.: Artech-House).

[3] Santos, J. L., Leite, A. P., and Jackson, D. A., 1992, *Appl. Optics*, **31**, 7361.

[4] Moslehi, B., Layton, M. R., and Shaw, H. J., 1989, *J. Lightwave Technol.*, **7**, 236.

[5] Capmany, J., 1992 *Optics Commun.*, **89**, 33.